AUTOMATIC CELL SEGMENTATION FROM CONFOCAL MICROSCOPY IMAGES OF THE ARABIDOPSIS ROOT

Monica Marcuzzo[1], *Pedro Quelhas*[1], *Ana Campilho*[3,4] *Ana Maria Mendonça*[1,2], *Aurélio Campilho*[1,2]

[1]INEB - Instituto de Engenharia Biomédica, Divisão de Sinal e Imagem, Campus FEUP
[2]Universidade do Porto, Faculdade de Engenharia
Departamento de Engenharia Electrotécnica e Computadores
[3]Department of Molecular Genetics, University of Utrecht

ABSTRACT

In vivo observation and tracking of cell division in the *Arabidopsis thaliana* root meristem, by time-lapse confocal microscopy, is central to biology research. The research herein described is based on large amount of image data, which must be analyzed to determine the location and state of cells. The possibility of automating the process of cell detection/marking is an important step to provide research tools to the biologists in order to ease the search for a special event as cell division. This paper discusses an automatic cell segmentation method, which selects the best cell candidates from a starting watershed based image segmentation. The selection of individual cells is obtained using a Support Vector Machine (SVM) classifier, based on the shape and edge strength of the cells' contour. The resulting segmentation is largely pruned of badly segmented cells, which can reduce the false positive detection of cell division. This is a good result on its own and a starting point for improvement of cell segmentation methodology.

Index Terms— Biomedical image processing, Image processing, Image segmentation, Biological cells

1. INTRODUCTION

Cell division in plants is greatly concentrated in specialized regions known as meristems [1]. In the *Arabidopsis*, the most important meristem is located at the tip of the root and perpetuates its pattern by cellular division. The stem cells, located in the root meristem, gives rise to all the cell types of the root by regular patterns of cell division. However, the mechanism by which cell division is controlled is not completely understood, what motivates *in vivo* research of plant cell division.

Development biologists studying roots find difficult to cope with the lack of suitable technology to analyze root meristem growth *in vivo* [1]. The great amount of data produced requires the development of image analysis tools to automatically extract useful information, such as identifying cell division and growth.

[4]Present address: Institute of Biotechnology, University of Helsinki

Many studies focus on the analysis of *Arabidopsis* development. Cell growth is analyzed using different approaches, such as mathematical models [2] and motion estimation methods [3]. The relation between cell division and elongation in the regulation of organ growth rate is also investigated [4]. These researches show that *in vivo* imaging of the root is a valuable tool. Furthermore, cell features should be extracted to be processed statistically, and an easy way to track these individual cells should be provided.

The first step for automated cell division identification is cell segmentation in the plant images. Segmentation is a difficult problem in computer vision and is, in this application, made worse by image acquisition process, data's variability and noise. There is a need for segmentation methodologies that can estimate the resulting segmentation's quality and use that knowledge to recover from errors. We present a step in that direction by designing a method that selects well segmented cells from a set of possible segmented regions.

This paper is organized as follows: Section 2 describes the *in vivo* image data acquisition. Section 3 describes the proposed approach. Section 4 presents and discusses the obtained results. Finally, conclusion is presented in Section 5.

2. IMAGE ACQUISITION

The database used in this work was obtained using an automated confocal microscope image-acquisition process. The motorized stage of the microscope is controlled to compensate the root's growth, as described in [5]. The time duration of the experiments ranged from 10 hours to more than a day, being images acquired every 10 minutes. To be able to acquire *in vivo* images of the plant root, Green Fluorescence Protein (GFP) markers were used to allow the visualization of the cell wall. When excited with a laser wavelength of its excitation spectrum, this protein emits light in the emission spectrum.

One problem with this type of image acquisition is the bleaching of the images caused by the degradation of the fluorescent protein compound (Fig.1). This degradation is caused by the laser flash used to image the cells and increases with

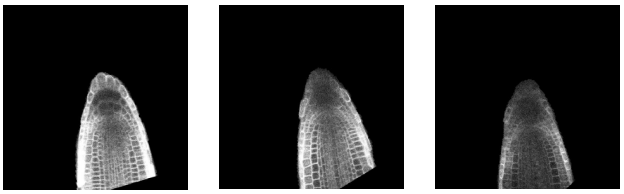

Frame 1 Frame 140 Frame 280

Fig. 1. Examples where the bleaching effect can be seen, specially in the center and in the tip of the root. As more images are collected, the contrast (and definition) decrease.

the number of exposures and the individual exposure time.

3. METHODOLOGY

In this section we present the proposed methodology to select the best cells from the segmentation of a plant image. Each possible region from the segmentation is classified based on the shape similarity to human selected cells' contours.

Our system has three main stages: image pre-processing, image segmentation and classification. Within each stage there are tasks that must be performed:

- Pre-processing: image registration and filtering;
- Segmentation: watershed segmentation, contour extraction and description;
- Classification: Support Vector Machine (SVM) contour classification.

This system is novel in its structure and introduces novel parts such as collaborative filtering and SVM cell contour classification.

3.1. Image registration

The direction of the root in the acquired images is not constant, due to the irregular growth of the root. However, for a similar description of the cell contours, we require the root to have the same approximate orientation in all the images. To obtain a normalized image I_r from each input image I with relation to rotation, we compute the central line of the root in the image and rotate the image so that the root is vertical with the tip in the upwards direction. The central line estimation is obtained using the method described by Garcia *et al*. [5].

3.2. Image Filtering

The images I resulting from confocal-microscopy have a high level of noise. This is a consequence of the reduced time of exposure, necessary to avoid excessive bleaching (Fig.1). To improve the quality of the images, prior to segmentation we need to use a noise filtering method. The resulting image I_{filt} will have a better level of information,

$$I_{filt} = \mathcal{F}(I_r, \sigma^2_{filt}), \quad (1)$$

where $\mathcal{F}$ is the noise reducing image filter and σ^2_{filt} is the variance of the assumed noise in the image. Larger σ^2_{filt} values will result in a smoother image, leading to a segmentation with fewer but larger regions (Fig.3). Two filtering methods were considered: anisotropic image filtering [6] and denoising by sparse 3D transform-domain collaborative filtering (BM3D) [7]. Visual inspection of results using both techniques in a large number of images led to the choice of the latter due to better results, see Figure 2.

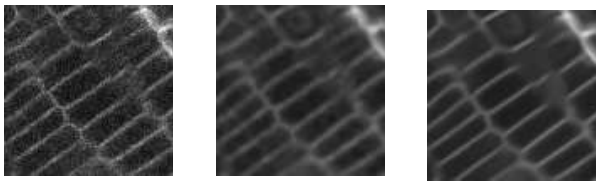

Noisy image Anisotropic Filt. BM3D Filt.

Fig. 2. Comparison of the result of filtering a noisy image with each different method (image crop detail). The BM3D [7] method eliminates more noise while better preserving image details.

3.3. Watershed segmentation

In order to segment the cells, we apply a watershed transform to the filtered images I_{filt}. The classical watershed transform is based on immersion simulation. The input gray-scale image is considered as a topographic surface which is flooded by water starting from regional minima. Watershed lines are formed on the meeting points of water coming from distinct minima [8]. The resulting segmentation is the set of n regions R_i $(i = 1, ..., n)$ obtained from the watershed transform.

Usually the direct application of the watershed transform to an image leads to over-segmentation. It is caused by the fact that there are more image minima than objects, that is, not all minima really represent true objects, due to noise [9]. In the *Arabidopsis* confocal images, cells have bright walls surrounding a dark non-homogeneous interior, which can lead to several minima inside a cell, resulting in over-segmentation.

Traditionally there are two strategies to reduce the over-segmentation problem. One tries to avoid the over-segmentation before it happens by limiting the number of allowable regions, often restricting the number of markers [9]. The other strategy allows over-segmentation to occur and then tries to repair it, usually by merging adjacent regions [10].

In the *Arabidopsis* confocal images, it is difficult to establish a strategy to avoid over-segmentation which remains valid for a whole experiment. This is due to the variability of the root size in the image and to the bleaching effect (shown in Fig.1). Any chosen approach can be adequate for the beginning of the biology experiment's data, however it can fail further on in the experiment. Our approach to this problem is to prune badly segmented regions after the segmentation step.

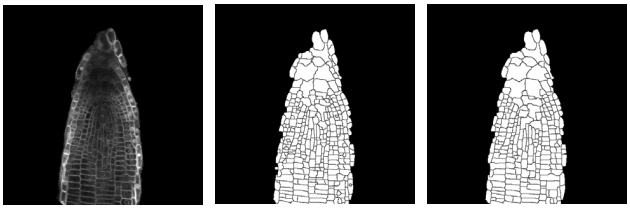

Original image σ_{filt} = 20 σ_{filt} = 40

Fig. 3. Watershed segmentation examples based on different filtering parameters of the original image.

3.4. Contour description

Using the watershed regions R_i derived in the previous step, we obtain the contour c_i of each region R_i by the extraction of its points, starting from the leftmost one in a clockwise order. To classify each contour we must first describe them. As such, we describe each region's contour by its shape and underlying image pixel's edge strength.The shape is characterized by the Discrete Cosine Transform (DCT) of the distance between each contour point and the contour's centroid. The edge strength at the contour's pixels is characterized by the phase symmetry measure [11]. This measure has the advantage of not producing double edges at line contours, and performs well in low contrast images. The contour descriptor vector is:

$$D_i = [DCT(\|c_i - centroid(c_i)\|) \quad PhSym(c_i)], \qquad (2)$$

where $\|c_i - centroid(c_i)\|$ is the vector of distances between each contour point and the contour's centroid, and $PhSym(c_i)$ is the Phase Symmetry measure of the pixels of the image at the contour coordinates. In order to have the same dimension for the obtained descriptor, we resample the contour to 40 points. This was found to describe the cell's shape with enough detail.

3.5. SVM Cell Classification

In order to prune the segmentation obtained with the watershed transform, we classify each region R_i into cell C_j or non-cell, based on its descriptor D_i, using a Gaussian kernel SVM [12]. The classifier training and testing is performed as follows:

Training: For each image, we applied the segmentation described in Sec.3.3, using different filtering sigmas σ_{filt} (see Sec.3.2). For each image we labeled segmentation regions that correspond to cells in the image and those which are clearly wrong (non-cell). We do not perform full annotation since some cases are ambiguous and it is more advantageous to gather better cell annotation from more images.

Testing: using the SVM model, given a new segmentation region's descriptor D_i, we can automatically classify that region as cell C_j or non-cell. Performing this operation for all regions in the image, we obtain an SVM pruned segmentation image with all the regions classified as cells (Fig.4(d)).

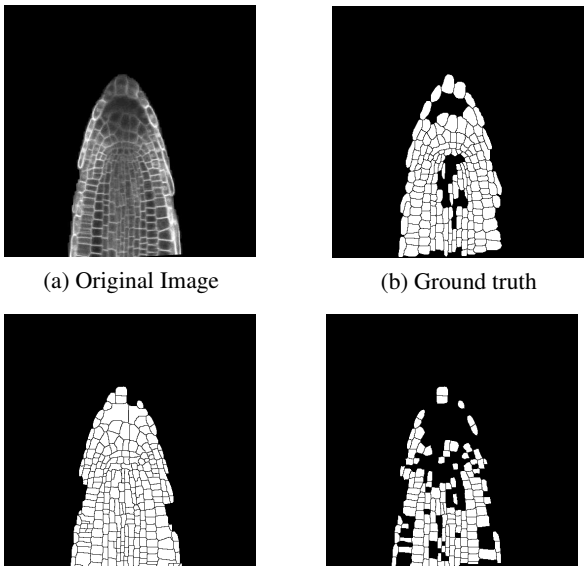

(a) Original Image (b) Ground truth

(c) Watershed segmentation (d) SVM pruned segmentation

Fig. 4. Original image and resulting segmentation obtained using the proposed method.

4. RESULTS AND DISCUSSION

We selected images from 16 biological experiments, from which 9 were used for training and 7 for test. In total, we used 68 images for training, containing 5125 manually selected cells. For test, 12 images were used, containing 1421 manual segmented cells, used as ground truth for evaluation of the method.

Applying the methodology described in the previous section we obtain an image with an SVM pruned cell segmentation (Fig.4(d)). In this section we compare the SVM pruned result with the direct result of the watershed segmentation (corresponding to all regions R_i being considered cells C_j).

For an objective evaluation of the cell segmentation results, we map each region classified as cell C_j to the best fitting ground truth region GT_k from the manual segmented image (Fig.4(b)). To obtain this mapping we use the F-measure, also known as coverage measure, defined by:

$$F(C_j, GT_k) = \frac{2\nu(C_j, GT_k)\rho(C_j, GT_k)}{\nu(C_j, GT_k) + \rho(C_j, GT_k)}, \qquad (3)$$

where ν is precision and ρ is recall, defined by:

$$\nu(C_j, GT_k) = \frac{C_j \bigcap GT_k}{C_j}, \quad \rho(C_j, GT_k) = \frac{C_j \bigcap GT_j}{GT_k} \quad (4)$$

Cell regions C_j are mapped to GT_k if the F-measure between them $F(C_j, GT_k)$ is above a certain threshold th. For the evaluation presented here, we consider $th = 0.6$. If there is one and only one cell region C_j mapped to a ground truth GT_k, we consider that cell region C_j as well classified. It is important to notice that, due to the poor image quality, the

Table 1. Comparison between the number of cells correctly returned by SVM classification and the watershed segmentation. Results for all cells in the 12 testing images. All numbers are averaged values over all images.

method	watershed			SVM		
σ_{filt}	20	30	40	20	30	40
F-measure	0.817	0.821	0.825	0.831	0.836	0.837
FP	156.7	123.5	107.5	61.7	57.3	51.1
FN	25.8	24.7	26.9	64.6	52.9	51.8
performance	0.38	0.43	0.46	0.51	0.55	0.56

ground truth annotation does not normally cover the whole root in the image (Fig.4(b)).

To objectively measure each approach's performance, we calculate several segmentation and classification measures:

- **F-measure:** evaluates the segmentation fitting;
- **False positive (FP), False negative (FN):** evaluates the type of classification errors;
- **Performance:** the ratio of correctly classified cells regions according to the ground truth.

All measures were calculated for each image and averaged over all images. The results are presented in Table 1.

We can conclude that, using our approach, we are able to greatly reduce false positives (at least 50% reduction) and create a segmentation which has a greater percentage of correctly segmented regions (at least 10% higher). It is also important to emphasize that we obtain an increase of the F-measure with the SVM pruned segmentation (1.5% approx.), even if it does not actually modify the segmentation of individual cells. This improvement in the F-number indicates that by using an SVM classifier we are able to correctly select the best cells.

5. CONCLUSION

In this work we introduced an approach to automatically select the segmentation of cells in plant confocal microscopy using an SVM classifier. Using this approach we are able to prune most of the wrongly segmented cells improving the performance of the resulting segmentation.

One major difficulty in this work is that the watershed segmentation from which we start contains a high percentage of miss-segmented cells, which we cannot recover from. Another point is that the SVM classifier does not take into account any information about the cell neighborhood. Future work will include a wrapper methodology in which we use the SVM classified cells to improve the base segmentation obtained with the watershed transform and include cell neighborhood information to improve classification.

ACKNOWLEDGEMENTS

The authors acknowledge the funding of Fundação para a Ciência e Tecnologia, under contract ERA-PG/0007/2006.

6. REFERENCES

[1] A. Campilho, B. Garcia, H. Toorn, H. Wijk, A. Campilho, and B. Scheres, "Time-lapse analysis of stem-cell divisions in the arabidopsis thaliana root meristem," *The Plant Journal*, vol. 48, pp. 619–627, 2006.

[2] A. Iwamoto, D. Satoh, M. Furutani, S. Maruyama, H. Ohba, and M. Sugiyama, "Insight into the basis of root growth in arabidopsis thaliana provided by a simple mathematical model," *J. Plant Res.*, vol. 119, pp. 85–93, 2006.

[3] T. Roberts, S. Mckenna, N. Wuyts, T. Valentine, and A. Bengough, "Performance of low-level motion estimation methods for confocal microscopy of plant cells in vivo," in *Motion07*, 2007, pp. 13–13.

[4] G. Beemster and T. Baskin, "Analysis of cell division and elongation underlying the developmental acceleration of root growth in arabidopsis thaliana," *Plant Physiology*, vol. 116, pp. 1515–1526, 1998.

[5] B. Garcia, A. Campilho, B. Scheres, and A. Campilho, "Automatic tracking of arabidopsis thaliana root meristem in confocal microscopy," in *Proc. of the Inter. Conf. on Image Analysis and Recognition*, 2004, pp. 166–174.

[6] P. Perona and J. Malik, "Scale-space and edge detection using anisotropic diffusion," *IEEE Trans. on PAMI*, vol. 7, no. 12, pp. 629–639, 1990.

[7] K. Dabov, A. Foi, V. Katkovnik, and K. Egiazarian, "Image denoising by sparse 3d transform-domain collaborative filtering," *IEEE Trans. on Image Processing*, vol. 16, no. 8, pp. 2080–2095, August 2007.

[8] V. Luc and P. Soille, "Watersheds in digital spaces: An efficient algorithm based on immersion simulations," *IEEE Trans. on PAMI*, vol. 13, no. 6.

[9] F. Meyer and S. Beucher, "Morphological segmentation," *JVCIR*, vol. 1, no. 1, pp. 21–46, Sept. 1990.

[10] A. Bleau and L. Leon, "Watershed-based segmentation and region merging," *Comput. Vis. Image Underst.*, vol. 77, no. 3, pp. 317–370, 2000.

[11] P. Kovesi, "Symmetry and asymmetry from local phase," in *Proc. of the Tenth Australian Joint Conf. on Artificial Intelligence*, December 1997.

[12] C. Burges, "A tutorial on support vector machines for pattern recognition," *Data Mining and Knowledge Discovery*, vol. 2, no. 2, pp. 121–167, 1998.